ELSEVIER

Sensors and Actuators A 62 (1997) 506–512

SENSORS AND ACTUATORS A PHYSICAL

Asymmetrical locations of heaters and sensors relative to each other using heater arrays: a novel method for designing multi-range electrocaloric mass-flow sensors

N.T. Nguyen *, W. Dötzel

Department of Electrical Engineering and Information Technology, Technical University of Chemnitz-Zwickau, D-09107 Chemnitz, Germany

Abstract

A novel and simple method for designing multi-range electrocaloric mass-flow sensors has been presented. This new method is based on the asymmetrical relative positioning of heaters and temperature sensors, which is realized by using an array of heaters or temperature sensors. A simple analytical model and a numerical model with FIDAP have been verified by experimental results. The method of asymmetrical locations extends the flexibility of a sensor chip. Different fluids and variable flow ranges can be measured by only one sensor chip without changing the design, operation modes or amplifier gain. © 1997 Elsevier Science S.A.

Keywords: Multi-range mass-flow sensors; Heat transfer; Forced convection; Electrocaloric principle; Silicon sensors

1. Introduction

Mass-flow measurement is nowadays an important field in process control. The measurement tasks and measured fluids are widely varied. Therefore, there is a need for a mass-flow sensor which can be used for different fluids and variable flow ranges. This purpose can be realized by using different operational modes with the same sensor chip [1]. This paper presents a new method for scaling the flow range in the operational mode 'constant heating power, evaluation of temperature difference' [1]. The expression 'temperature difference' is used in this paper to indicate the temperature difference between thermal sensors positioned up- and downstream of the heater.

In recent years, many mass-flow sensors have been developed and published. Most of them are based on the above-mentioned operational mode. The temperature sensors were realized by using different transducing principles: thermoresistive (metal or silicon resistors) [2–4], thermoelectric (thermopiles) [5–9] and thermoelectronic (transistors or diodes) [10,11]. All these reported mass-flow sensors have only one heater resistor and two temperature sensors. Therefore they only work in the flow range that is determined by the distance between the heater and temperature sensors. Our sensor has a heater array of three elements and a temperature-sensor array of four elements, as shown in Fig. 1(a) [1]. In this paper, the heater array and two of the temperature sensors are investigated by using the method of asymmetrical locations of heaters and sensors relative to each other (Fig. 1(b)). This method can be realized by activating one or two elements of the heater array. The new method gives the flexibility of different flow ranges with only one sensor chip.

2. The mass-flow sensor

The electrocaloric mass-flow sensor is based on the thermoresistive principle. The fluid flow modulates the temperature distribution on the sensor diaphragm. The displacement of the temperature profile can be detected by integrated temperature sensors located up- and downstream of the heater. In our mass-flow sensor, silicon resistors are used for heating and sensing functions.

Because of the small specific resistance and a small thermoelectric Seebeck coefficient, the meander-shaped metal resistors [3,4,13] and thermopiles require a large lateral area [5–11]. In contrast with the above-mentioned temperature sensors, the resistance of implanted silicon and its temperature coefficient can be modulated by technology parameters. Therefore a small resistor structure and a miniaturized mass-flow sensor can be made by using integrated silicon resistors (poly- or single-crystalline silicon).

* Corresponding author. Tel.: +49 371 531 3274. Fax: +49 371 531 3259. E-mail: ntn@infotech.tu-chemnitz.de

PII S0924-4247(97)01529-X

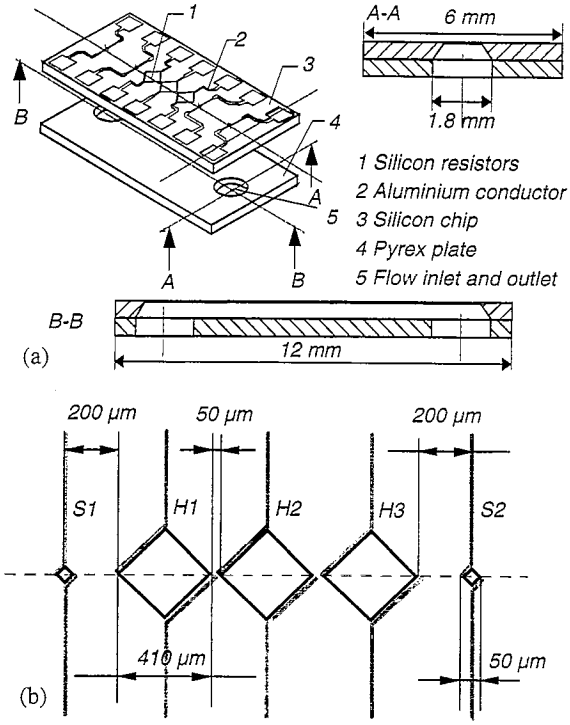

Fig. 1. The multi-range electrocaloric mass flow sensor: (a) perspective view; (b) heater array and temperature sensors of the flow sensor.

The operational modes of the mass-flow sensor and its technology were reported in Ref. [1]. We started with a {100}-oriented silicon wafer polished on both sides. Polysilicon or single-crystalline silicon resistors were made with standard processes. Aluminium was deposited as an electrical conductor. After the fabrication of resistor and conductor structures and the protecting silicon nitride passivation layer, the microchannel was formed by anisotropic etching of silicon in KOH solution (80%, 30°C). The channel is covered by anodic bonding to a glass plate or gluing directly on a supporting substrate, Fig. 1(a). The fluid-flow channel cross section has a typical trapezoidal shape. The heater array consists of three resistors located on a thin diaphragm which has a thickness d_M of 15 to 30 µm. The electrical supply was realized by using wire bonding contacts. The geometry of the heater array and the temperature sensors is shown in Fig. 1.

3. Method of asymmetrical locations

Fig. 2 shows the temperature distribution on the sensor diaphragm without flow (Fig. 2(a)) and with a 29.4 ml min^{-1} water flow (Fig. 2(b)). The measurement was carried out by using a thermography system. The three heater resistors lie between B and C. The temperature sensors could be located symmetrically (A and D) or asymmetrically (E and D).

Without flow, the temperature profile is symmetrical. We find $\Delta T_{AD}=0$ and $\Delta T_{ED}=\Delta T_0$. A fluid flow in the sensor channel displaces the temperature profile on the diaphragm.

For low flow rates and constant heat power, the temperature difference ΔT_{AD} is linear with flow rate; it reaches a maximum and decreases with increasing flow rate [1,4,14] (Fig. 3). The flow rate at which the maximum occurs can be changed by varying the distance between sensors and heater [4,12] or by using an integrated heat sink and flow guide [13]. On the other hand, the difference $\Delta T_{ED}-\Delta T_0$ also decreases for high flow rate because of the relatively low temperature at point E (Fig. 2). As a results, the flow rate at which the maximum output occurs, and hence the operational flow range, can be changed by using asymmetrical locations of the upstream and downstream temperature sensors with respect to the heating source. The asymmetrical locations can be flexibly realized by using arrays of heaters or temperature sensors. Alternatively, because of the comparatively large geometry required by meander-shaped resistors or thermopiles, it may be more favourable to use asymmetrical locations of the heating source with fixed temperature-sensor locations.

In our mass-flow sensor, the asymmetrical locations are realized by combining the three elements H1, H2 and H3 of the heater array shown in Fig. 1. The temperature difference is measured by up- and downstream sensor elements S1 and

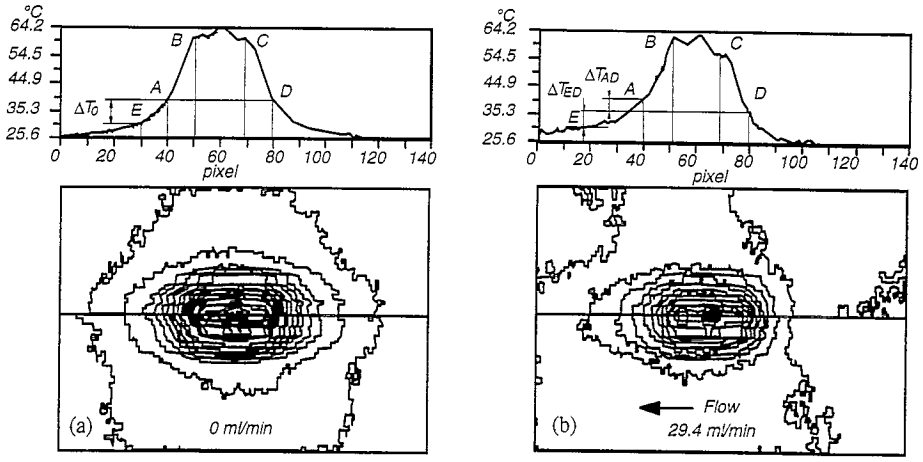

Fig. 2. Temperature distribution on the sensor diaphragm (a) without flow, (b) with flow.

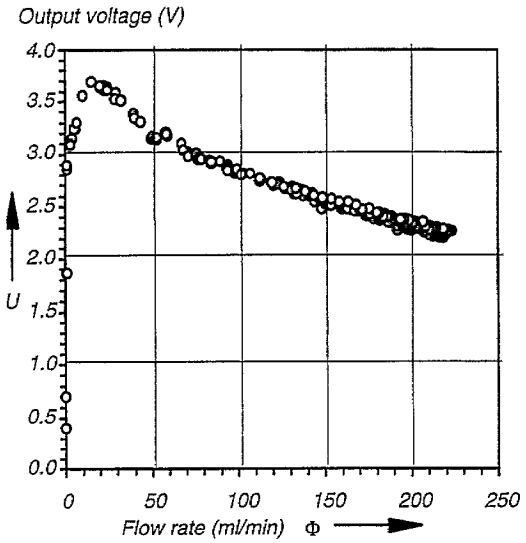

Fig. 3. Characteristics of the temperature difference using symmetrical locations of temperature sensors [1].

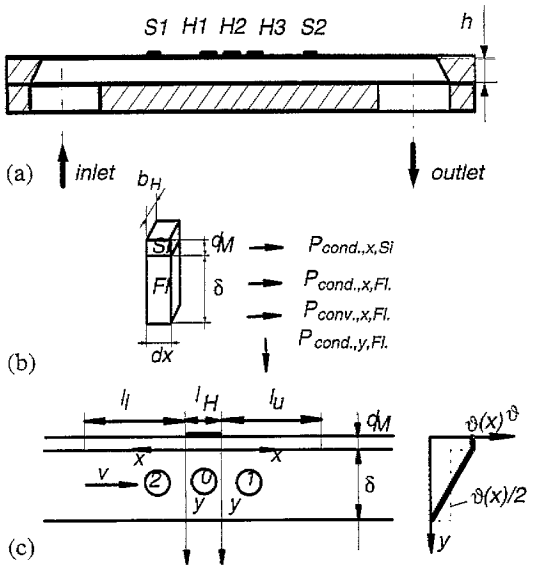

Fig. 4. Model of the sensor: (a) cross section along the channel; (b) lumped element for analytical analysis; (c) geometrical definition of the model.

S2 positioned in a half-bridge circuit. The initial temperature difference ΔT_0 is compensated by using an external low-impedance potentiometer. The other part of the circuit is a differential-input instrumentation amplifier [3].

4. Analytical model

A simple one-dimensional model is used to show the working principle of the asymmetrical locations. Geometrical parameters and assumptions are given in Table 1 and Fig. 4.

The conservation of thermal energy in a lumped element (Fig. 4(b)) can be given in the following equation:

$$P_{\text{cond.,x,fluid}} + P_{\text{conv.,x,fluid}} + P_{\text{cond.,x,Si}} = P_{\text{cond.,y,fluid}} \tag{1}$$

The indices define the conduction or convection in the x- or y-direction in the fluid as well as in the silicon diaphragm. With the temperature along the x-axis $\vartheta(x)$, the average flow velocity v, the thermal conductivities of silicon λ_{Si} and of fluid λ_{Fl}, the thermal diffusivity of fluid a_{Fl} and the constant thickness of the thermal boundary layer δ we find the heat-balance equation:

Table 1
Geometrical parameters of the model

Parameter	Term	Value
Channel height	h	500 μm
Heater length (sym., $l_u = l_l$)	l_H	1330 μm
Heater width	b_H	410 μm
Diaphragm thickness	d_M	20 μm
Distance (asym., $l_u > l_l$)	l_u, l_l	660, 200 μm
Cross-section area	A	0.682 mm^2

$$-\lambda_{Fl}\frac{\vartheta(x)}{2dx}b_H\delta + \rho_{Fl}c_{Fl}v\frac{\vartheta(x)}{2} - \lambda_{Si}\frac{\vartheta(x)}{dx}b_H d_M = \lambda_{Fl}\frac{\vartheta(x)}{\delta}b_H dx \tag{2}$$

or in the form of a differential equation:

$$\left(\frac{1}{2} + \frac{\lambda_{Si}d_M}{\lambda_{Fl}\delta}\right)\frac{\partial^2\vartheta(x)}{\partial x^2} - \frac{v}{2a_{Fl}}\frac{\partial\vartheta(x)}{\partial x} - \frac{1}{\delta^2}\vartheta(x) = 0 \tag{3}$$

The thickness of the thermal boundary layer δ depends on the flow velocity [15]. In this model, the thermal boundary layer is assumed to be constant. For liquids with a large Prandtl number ($Pr \gg 1$), the thickness δ can be calculated by using an average Nusselt number from [16]

$$\delta = \frac{h}{2\left[83.326 + \left(1.9533\sqrt{\frac{vh^2Pr_{Fl}}{\nu_{Fl}l_H}} - 0.6\right)^3\right]^{1/3}} \tag{4}$$

In (4), ν_{Fl} is the kinematic viscosity of the fluid. For gases with a small Prandtl number ($Pr < 1$) or liquids with a low Reynolds number we can assume

$$\delta = h \tag{5}$$

After solving Eq. (3) in the local coordinate systems 1 and 2 (Fig. 4(c)) we get the temperature difference $\Delta\vartheta(v)$ between the temperature sensors:

$$\Delta\vartheta(v) = \vartheta_0[\exp(\gamma_2 l_u) - \exp(-\gamma_1 l_l)] \tag{6}$$

with

$$\gamma_{1,2} = \frac{v \pm \sqrt{v^2 + 16a_{Fl}^2\kappa/\delta^2}}{4a_{Fl}\kappa} \tag{7}$$

The dimensionless factor

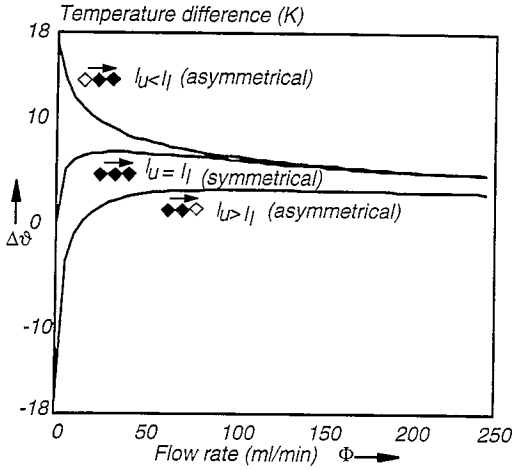

Fig. 5. Temperature difference as a function of water flow ϕ by using symmetrical (◆ ◆ ◆: $l_u = l_l = 200$ μm) and asymmetrical (◆ ◆ ◇: $l_u = 660$ μm, $l_l = 200$; ◇ ◆ ◆: $l_u = 200$ μm, $l_l = 660$) locations.

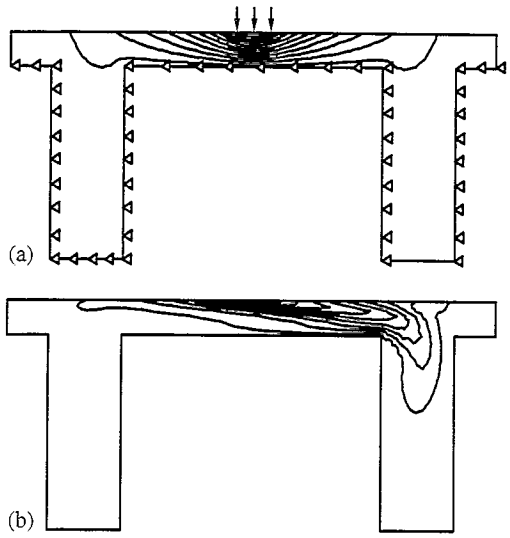

Fig. 6. Results of numerical simulation by using FIDAP (a) without flow (triangle, fixed ambient temperature; arrow, heat flux); (b) with flow (the temperature profile inside the channel is displaced in the flow direction).

$$\kappa = \frac{1}{2} + \frac{\lambda_{Si} d_M}{\lambda_{Fl} \delta} \tag{8}$$

describes the influence of the silicon diaphragm on the heat balance. If the heat conduction in the silicon diaphragm is neglected, we get $\kappa = 1/2$ as in the similar case of Ref. [4].

The heater temperature ϑ_0 can be calculated for the constant heat power P:

$$\vartheta_0 = \frac{P}{\lambda_{Fl} b_H [l_H/\delta + \sqrt{(v^2\delta^2)/(4a_{Fl}^2) + 4\kappa}]} \tag{9}$$

Fig. 5 shows the results of this analytical model. The heating elements of the array are designated by black filled symbols. The advantage of the asymmetrical locations is clearly illustrated by the analytical results. A high temperature difference and different sensor characteristics can be achieved by using this method.

For designing a thermal flow sensor, this analytical model is not suitable because of the imprecise assumptions (4) and (5). In reality, the thermal boundary layer is not invariable along the flow direction (compare with the results of numerical simulation in Fig. 6) and depends on the three-dimensional geometry of the sensor. The numerical simulation with a two-dimensional model yields better results.

5. Numerical simulation

The numerical simulation of the fluid and thermal flow in the electrocaloric mass-flow sensor was realized by FLOTRAN or FIDAP. In this paper, results with FIDAP are presented. The CFD program FIDAP is able to solve the coupled field of flow and temperature. The three balance equations:— of mass conservation:

$$\frac{\partial \rho}{\partial t} + \nabla \cdot (\rho v) = 0 \tag{10}$$

– of momentum conservation (Navier–Stokes equations):

$$\rho \frac{\partial v}{\partial t} + v \cdot \nabla v = -\nabla p + \eta \nabla^2 v \tag{11}$$

– and of energy conservation:

$$\frac{\partial \vartheta}{\partial t} + v \nabla \vartheta = \frac{\lambda}{\rho c} \nabla^2 \vartheta \tag{12}$$

can be solved together. In our case, the Navier–Stokes equations and the continuity equation are solved first. In the next step, the calculated velocity field can be used as the boundary condition for solving the energy equation. This method is valid only under the assumption that the fluid properties do not depend on the temperature. It allows a convenient computing time.

We assumed that the model of the sensor is two dimensional. The laminar model is in use. The setting of room temperature as a boundary condition is not symmetrical in the model because of the undefined temperature field on the downstream side of the sensor (Fig. 6(a)). A constant heat rate was applied to the heater of the model. The inlet is fixed by a constant flow velocity. The results of the temperature distribution are shown in Fig. 6.

6. Experimental results

6.1. Results of water flow

6.1.1. Results in the high flow range (ml min^{-1})

The experimental set-up was described in Ref. [1]. The measurements were carried out automatically by using a computer and the programming tool Labview. It allows program-

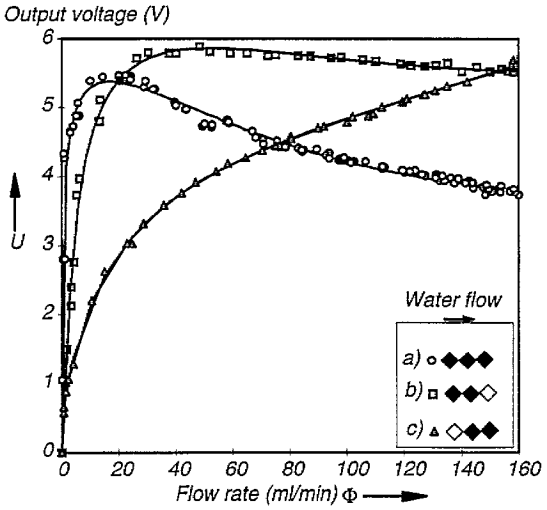

Fig. 7. Output voltage of the sensor (amplified, offset compensated and inverted (c), black filled squares represent the active heater elements, the solid lines are the approximated functions of the measurement points).

mable measuring and automatic recording of experimental results. The measurements were done with water at a temperature of 25°C. The heating power is kept constant at 600 mW. A amplifier circuit with a Wheatstone bridge is used for measuring the temperature difference between the downstream and the upstream sensors. In the case of asymmetrical locations, the offset of the bridge voltage was compensated before amplification.

With this experimental set-up the first measurements near zero flow are very unstable because of the high sensitivity in this range. Detailed investigations in the low flow range are dealt with in Section 6.1.2.

The sensor characteristics of the symmetrical locations are shown in Fig. 7. The maximum of the output voltage is reached at a flow of approximately 10 ml min^{-1}. The sensor characteristic does not depend on the flow direction.

With the asymmetrical locations, the influence of the positions of heater elements is clearly illustrated in the characteristics of the sensor output (Fig. 7). The experimental results agree with the results of the analytical model shown in Fig. 5.

6.1.2. *Results in the low flow range (μl min^{-1})*

The measurement in this range was carried out with the MICMEC group (University of Twente). The small flow is generated by a commercial syringe which is driven by a stepper motor. A maximum water flow of 25 μl min^{-1} could be created. The experiments were carried out at a room temperature of 25°C. The bridge voltage was measured directly. Fig. 8 compares the measurement with the numerical simulation. The sensitivity of the bridge voltage decreases by using the asymmetrical locating without changing other conditions (compare the linear function approximation of the measured bridge voltage in Fig. 8(a) and (b)). With the arrangement in Fig. 8(c), the curve becomes non-linear.

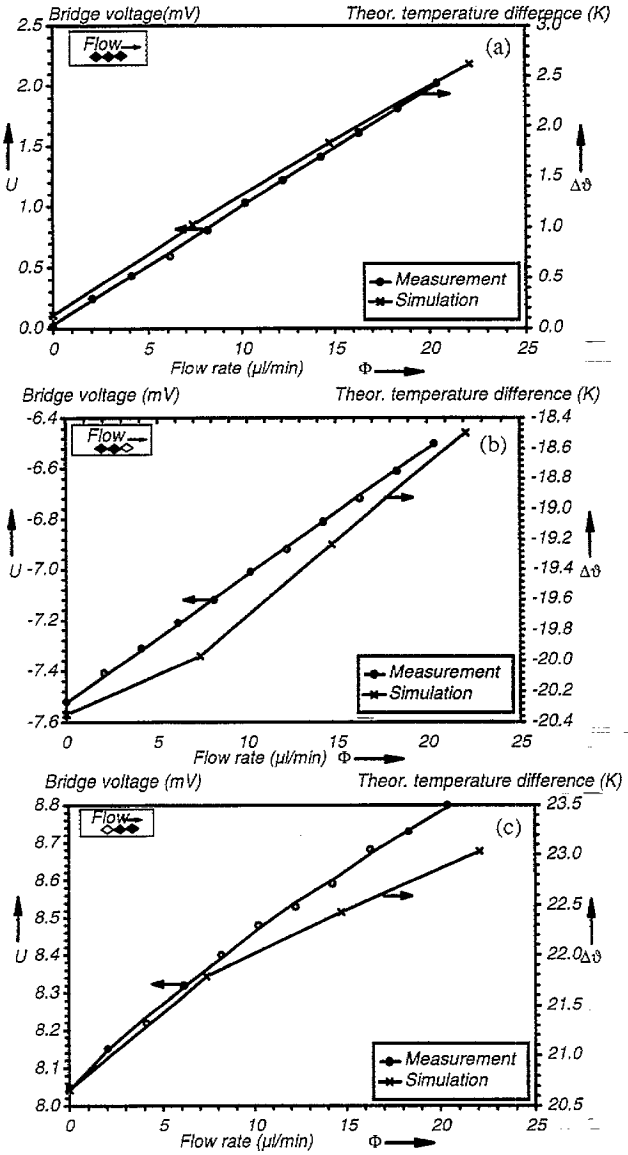

Fig. 8. Bridge voltage vs. the flow rate (water, black filled squares represent the active heater elements): (a) symm., $U = 0.0974\Phi + 0.025$; (b) asymm., $U = 0.0493\Phi - 7.5159$; (c) asymm., $U = 2E-5.\Phi^3 - 0.001\Phi^2 + 0.0495\Phi + 8.0486$.

6.2. *Results of nitrogen flow*

The same experiment as in Section 6.1.2 was carried out for nitrogen flow. A nitrogen flow from 0 to 60 ml min^{-1} can be created by using a flow controller of BRONKHOST F-100C/F-200C series. The results show clearly the dependency of the bridge-voltage curve shape on the arrangement of heater elements.

The general behaviour of the sensor characteristics for nitrogen flow in this range is similar to the results for water in the low flow range. With the arrangement in Fig. 9(b), we get a linear sensor characteristic. We can see in this example that with only one sensor chip three different measurement ranges could be realized (small, Fig. 9(c); medium, Fig. 9(a) and large, Fig. 9(b)).

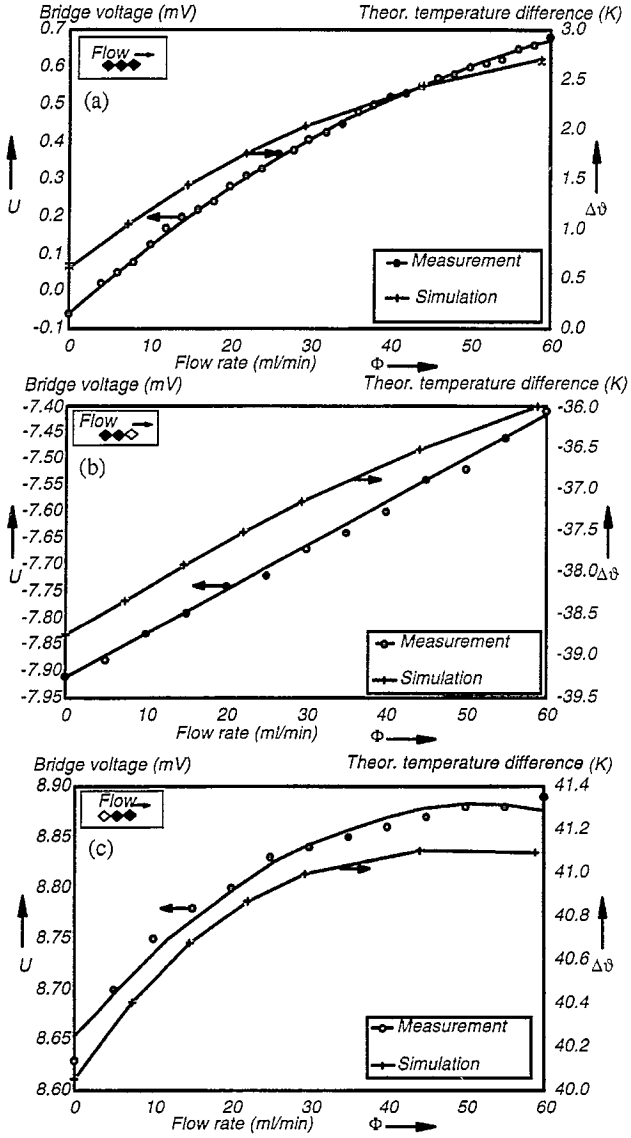

Fig. 9. Bridge voltage vs. the flow rate (nitrogen, black filled squares represent the active heater elements): (a) symm., $U = 1E-6.\Phi^3 - 2E-4.\Phi^2 + 0.0206\Phi - 0.0585$; (b) asymm., $U = 0.0082\Phi - 7.9156$; (c) asymm., $U = -9E-5.\Phi^2 + 0.009\Phi + 8.6525$.

7. Conclusions

A novel method for scaling electrocaloric mass-flow sensors has been analytically and numerically calculated, and verified by experimental results. The method is based on the asymmetrical locations of sensor elements. This method is realized by using a heater array. The results show the simple possibility to design a multi-range electrocaloric mass-flow sensor which is suitable for measuring different gases and liquids.

Acknowledgements

A part of this work was supported by the Sächsisches Staatsministerium für Wirtschaft und Arbeit (Saxony, Germany), contract no. 0045/009. The authors thank Dr Kiehnscherf and colleagues at the Center of Micro-Technology, Technical University of Chemnitz-Zwickau, for their assistance and contribution. One of the authors (N.T. Nguyen) thanks Dr Th. Lammerink and other colleagues of the MIC-MEC-group of the MESA Institute at the University of Twente (The Netherlands) for their supervision and assistance during his stay there from March to May 1996.

References

[1] N.T. Nguyen and R. Kiehnscherf, Low-cost silicon sensors for mass flow measurement of liquids and gases, *Sensors and Actuators A, 49* (1995) 17–20.

[2] R. Kiehnscherf, N.T. Nguyen and M. Schulze, Elektrokalorischer Durchflußmengensensor für Gase und Öle, *F and M Feinwerktechnik Mikrotechnik Messtechnik, 9* (1994) 402–406.

[3] R.G. Johnson and R.E. Egashi, A highly sensitive silicon chip microtransducer for air flow and differential pressure sensing applications, *Sensor and Actuators, 11* (1987) 63–67.

[4] T.S.J. Lammerink, N.R. Tas, M. Elwenspoek and J.H.J. Fluitman, Micro-liquid flow sensor, *Sensors and Actuators A, 37–38* (1993) 45–50.

[5] B.W. van Oudheusden and J.H. Huijsing, Integrated flow friction sensor, *Sensors and Actuators, 15* (1988) 135–144.

[6] B.W. van Oudheusden, The thermal modelling of a flow sensor based on differential convective heat transfer, *Sensors and Actuators, 29* (1991) 93–106.

[7] B.W. van Oudheusden, Silicon thermal flow sensors, *Sensors and Actuators, 30* (1992) 5–26.

[8] D. Moser and H. Baltes, A high sensitivity CMOS gas flow sensor on a thin dielectric membrane, *Sensors and Actuators A, 37–38* (1993) 33–37.

[9] K. Fricke, A micro machined mass-flow sensor with integrated electronics on GaAs, *Sensors and Actuators A, 45* (1994) 91–94.

[10] C. Yang and H. Soeberg, Monolithic flow sensor for measuring millilitre per minute liquid flow, *Sensors and Actuators A, 33* (1992) 143–153.

[11] R. Kersjes, J. Eichholz, A. Langerbein, Y. Manoli and W. Mokwa, An integrated sensor for invasive blood-velocity measurement, *Sensors and Actuators A, 37–38* (1993) 674–678.

[12] I. Mayer, O. Paul and H. Baltes, Influence of design geometry and packaging on the response of thermal CMOS flow sensors, *Tech. Digest, 8th Int. Conf. Solid-State Sensors and Actuators (Transducers '95/Eurosensors IX), Stockholm, Sweden, 25–29 June, 1995*, pp. 528–531.

[13] L. Qiu, E. Obermeier and A. Schubert, A microsensor with integrated heat sink and flow guid for gas flow sensing applications, *Tech. Digest, 8th Int. Conf. Solid-State Sensors and Actuators (Transducers '95/Eurosensors IX), Stockholm, Sweden, 25–29 June, 1995*, pp. 520–523.

[14] F.J. Auerbach, G. Meiendres, R. Müller and G.J.E. Scheller, Simulation of the thermal behaviour of thermal flow sensors by equivalent electrical circuits, *Sensors and Actuators A, 41–42* (1994) 275–278.

[15] H. Schlichting and K. Gersten, *Grenzschicht-Theorie*, Vol. 9, Springer, Berlin, 1996, p. 257.

[16] *VDI-Wärmeatlas*, VDI, Weinheim, 1993.

Biographies

Nam-Trung Nguyen was born in Hanoi, Vietnam, in 1970. He received the Dipl.-Ing. degree in electronic engineering

from the Technical University Chemnitz-Zwickau, Germany, in 1993. He is currently working as a research assistant in the Microsystem and Device Engineering Group of the Department of Electronic Engineering and Information Technology at the same university, where he is engaged in research on micromechanical flow sensors and microfluid systems. He has just finished his Ph.D. thesis on this research field.

Wolfram Dötzel was born in Erfurt, Germany, in 1941. He received the Dipl.-Ing. degree in electrical and precision engineering from Technical University Dresden in 1966 and the Dr.-Ing. degree from the Technical University Karl-Marx-Stadt (Chemnitz) in 1971. In 1973 he worked at the Energetic Institute in Moscow on the reliability of electromechanical systems. From 1974 to 1986 he worked in the field of peripheral computer equipment. Since 1987 he has been involved with the research and development of micromechanical components. Since 1993 he has been a professor of microsystem and device technology at the Technical University Chemnitz-Zwickau. His current work is focused on design and simulation of micromechanical structures and their application, especially in precision engineering.